Chinese Chemical Letters 33 (2022) 1245–1253

Contents lists available at ScienceDirect

Chinese Chemical Letters

journal homepage: www.elsevier.com/locate/cclet

Quantum dots-hydrogel composites for biomedical applications

Wenjie Zhou[a,1], Zhe Hu[a,1], Jinxin Wei[a], Hanqing Dai[b], Yuanyuan Chen[a], Siyu Liu[b], Zhongtao Duan[b], Fengxian Xie[a], Wanlu Zhang[a,*], Ruiqian Guo[a,b,c,d,*]

[a] Institute for Electric Light Sources, School of Information Science and Technology, Fudan University, Shanghai 200433, China
[b] Institute of Future Lighting, Academy for Engineering and Technology, Fudan University, Shanghai 200433, China
[c] Zhongshan-Fudan Joint Innovation Center, Zhongshan 528437, China
[d] Yiwu Research Institute of Fudan University, Yiwu 322000, China

ARTICLE INFO

Article history:
Received 13 May 2021
Revised 4 September 2021
Accepted 6 September 2021
Available online 10 September 2021

Keywords:
Quantum dots
Hydrogels
Bioimaging
Biosensing
Drug delivery

ABSTRACT

Quantum dots-hydrogel composites are promising new materials that have attracted extensive attention due to their incomparable biocompatibility and acceptable biodegradability, leading to enormous potential applications for various fields. This review summarizes the recent advances in quantum dots-hydrogel composites with a focus on synthesis methods, including hydrogel gelation in quantum dots (QDs) solution, embedding prepared QDs into hydrogels after gelation, forming QDs *in situ* within the preformed gel and cross-linking *via* QDs to form hydrogels. In particularly, biomedical applications as bioimaging, biosensing and drug delivery are also reviewed, followed by a discussion on the inherent challenges of design optimization, biocompatibility and bimodal applications and the prospect of the future development. These results will guide the development of quantum dots-hydrogel composites and provide critical insights to inspire researchers in future.

1. Introduction

Hydrogels, 3D polymeric network with porous structures and large amounts of water, have been extensively used as wound dressings, contact lenses, medical adhesives, and tissue engineering scaffolds over the last few decades [1-5]. Hydrogels can be divided into two categories by type of cross-linking [6,7]. Polymeric hydrogels are those networks crosslinked by covalent bonds, while supramolecular hydrogels are formed *via* physical association between polymeric chains or nanoparticles, such as hydrophobic interaction, hydrogen bonds, charge interaction [8,9]. Polymeric hydrogels are the main substrates of quantum dots-hydrogel (QDs-hydrogel) composites introduced in this paper, which can be classified as natural hydrogels, synthetic hydrogels and semi-synthetic hydrogels [10]. By comparison, the supramolecular interactions endow supramolecular hydrogels with better thixotropy, degradability and shear-thinning properties, while polymeric hydrogels are of higher mechanical strength, better stability, and lower cost [9]. Since Wichterle and Lim [11] prepared the first hydrophobic gel in 1960s for biological uses, the number of scientific publications related to hydrogels increased rapidly due to their good biocompatibility and acceptable biodegradability [12-15].

Moreover, some nanoparticles are embedded into hydrogels to expand their application, such as quantum dots (QDs) [16], fluorescent dyes [17] and gold/silver nanoparticles [18]. Due to the diverse properties of nanoparticles, the nanoparticles-hydrogel composites possess a structural diversity and property enhancement rather than individual materials [19-22]. QDs are colloidal nanocrystalline semi-conductors with unique fluorescent properties that, have attracted much attention since first prepared in 1981 [23-25]. In general, QDs can be divided into two categories as inorganic and carbon-based QDs. Inorganic QDs include III-V QDs [26], II-VI QDs [27], alloying QDs [28], *etc.* Carbon-based QDs are represented by carbon quantum dots (CQDs) and graphene QDs (GQDs) [29-31]. In biomedical applications, QDs are of excellent optical properties and better stability than fluorescent dye molecules [3], which leads to brighter imaging with both better thermal and chemical stability. Besides, QDs are more feasible for surface modification to be suitable for biological systems.

Compared to the individual components, the embeddedness of QDs into hydrogels endows the composites unique properties. Some QDs quench in fluorescence due to aggregation, which requires surface modifications or being embedded into the matrix for recovery. The stability and biocompatibility of hydrogels make them a preferred substrate for QDs composites in biological imag-

* Corresponding authors.
E-mail addresses: fdwlzhang@fudan.edu.cn (W. Zhang), rqguo@fudan.edu.cn (R. Guo).
[1] These authors contributed equally to this work.

https://doi.org/10.1016/j.cclet.2021.09.027
1001-8417/

Fig. 1. Schematic of QDs-hydrogel composites and their biomedical applications.

ing. On the other hand, the combination of stimuli-responsive hydrogels and QDs makes it possible for stimuli-responsive optical biosensing. In drug delivery, QDs are used for fluorescent tracing of the drug. However, the limited surface of QDs leads to a low drug loading efficiency, and most of the QDs possess a poor sensitivity to the changes of the internal environment. Hydrogels can be the substrates to significantly increase drug loading efficiency and sensitivity, also providing mechanical and chemical stability for QDs [32]. Relatively, the introduction of QDs also increases its mechanical stability to a certain extent, achieving a win-win situation [33]. Thus, QDs-hydrogel composites show great potential for biomedical applications especially as presented in Fig. 1.

The combination of various QDs with hydrogels endows the composite with their own advantages and disadvantages. Inorganic QDs are of better optical properties. For example, the tunable emission of alloying QDs can be applied to prepare hydrogels of tunable fluorescence. Compared to carbon-based QDs, inorganic QDs are more widely used in the new fluorescence detection technique of Förster resonance energy transfer biosensors, which provides the inorganic QDs-hydrogel composites a higher sensitivity. However, some cadmium-containing inorganic QDs are of higher toxicity like CdTe and CdSe QDs, so the toxic QDs are usually encapsulated inside the hydrogels or fixed *in-situ* on the surface of hydrogels through the covalent or non-covalent bonding between surface functional groups of QDs and hydrogel chains [34-36]. Another strategy is to coat the QDs with the shell to avoid the leakage of Cd^{2+} to reduce the toxicity of the individual materials [37].

In comparison with inorganic QDs, the toxicity of carbon-based QDs are much lower, and carbon-based QDs are more feasible for surface functionalization [31,38,39]. Thus, the abundant functional groups on the surface can be readily conjugated with molecular recognition elements. The features are vital in biomedical applications, which not only endow carbon-based QDs with better biocompatibility but also provide better targeting ability.

This review will focus on QDs-hydrogel composites for their excellent properties and vital role in biomedical field. In short, we have summarized the synthesis of the structurally-diverse QDs-hydrogel composites and their applications in biomedical field including biosensing, bioimaging and drug delivery. Furthermore, the challenge and outlooks of developing these materials for biomedical applications will be presented. We expect that it will provide a profound understanding of the QDs-hydrogel composites and inspire researchers to appropriately develop new composites as desired for biomedical applications.

2. Synthesis of QDs-hydrogel composites

Homopolymers or copolymers are used to prepare hydrogels *via* chemically or physically cross-linking to endow them with specific mechanical and chemical characteristics [40]. Various QDs-hydrogel composites have been prepared by embedding diverse QDs into the bulk hydrogel framework [41-43]. To acquire uniform distribution, several main methods have been employed, such as hydrogel gelation in QDs solution (Fig. 2a), embedding prepared QDs into hydrogels after gelation (Fig. 2b), forming QDs *in situ* within the preformed gel (Fig. 2c) and cross-linking *via* QDs to form hydrogels (Fig. 2d).

2.1. Hydrogel gelation in a QDs solution

The simplest way to acquire QDs-hydrogel composites is to form the hydrogels in a QDs solution. Park *et al.* [44] prepared a tyrosinase-QDs conjugates hydrogel composite by adding a tyrosinase-QDs conjugate solution into the monomer mixture. With exposure to ultraviolet light, highly cross-linked networks were formed due to the free-radical polymerization of methacrylate groups of poly(2-hydroxyethyl methacrylate) and poly(ethylene glycol) dimethacrylate, capable of entrapping the tyrosinase-QDs conjugate. Zhou *et al.* [45] also adopted this approach to obtain hydrogels embedded with CdTe QDs using $[(CH_3O)_3Si(CH_2)_2N^+(CH_3)_2C_{18}H_{37}Cl^-]$ (DC5700) as coupling agent, followed by the mixture with a variety of anion solutions and prepared CdTe QDs (Fig. 3a). Due to the sensitivity of the siloxane group to fluoride ion, a rapid sol-gel transition can be observed when induced by fluoride ion as shown in Fig. 3b, marking the formation of the hydrogel. However, the mixture remained a sol when added to other anion solutions, so such a technique may provide a new method to sense fluoride ion through sol-gel transition. Despite the convenience, this method has an obvious drawback that the QDs may exudate from the hydrogel matrix in case of low crosslinking density [46].

2.2. Embedding prepared QDs into hydrogels after gelation

Another way is to embed prepared QDs into hydrogels after gelation. Martin *et al.* [47] developed an approach to incorporate GQDs into hydrogels after gelation for application in polyaromatic molecules detection. The prepared cross-linked hydrogels were dried and immersed in a GQDs solution to load with GQDs (Fig. 4a). The electrostatic interactions enabled GQDs to remain anchored in the hydrogels (Figs. 4b and c). The final composite proved to be stable after swelling-deswelling cycles for several times and remained unaltered within a wide pH range in contrast to the GQDs solution. Besides electrostatic interactions, ultrasonic treatment is another way to achieve physical incorporation. Yang *et al.* [48] constructed multifluorescent hydrogels by QDs and polypeptide-engineered. The $PC_{10}A$ nanogels were first prepared by hydrophobic coiled-coil aggregates of the terminal P and A domains in $PC_{10}A$ polypeptide. The CdSe@ZnS QDs underwent a phase transfer process through encapsulated with $PC_{10}A$ nanogels. When solubilized into a high concentration of $PC_{10}A$, the oil-soluble can incorporate the hydrophobic area of $PC_{10}A$ nanogels by ultrasonic force. However, the easy loading of QDs also means the easy leakage, leading to the increase of biotoxicity, thus the low stability has been a great limitation of the biomedical applications.

2.3. Forming QDs in situ within the preformed gel

To form the QDs in the preformed gel is also employed in the preparation of QDs-hydrogel composites. Instead of embedding the prepared QDs, the approach involves loading the precursors into the hydrogel first. Sahiner *et al.* [49] reported an approach to prepare CdS QDs using hydrogel network as a template. In a typical process, a crosslinked hydrophilic hydrogel was first prepared using 2-acrylamido-2-methyl-1-propansulfonic acid (AMPS) monomers and cross linker *N,N′*-methylenebisacrylamide *via* photo-polymerization technique. Due to the anionic characteristic,

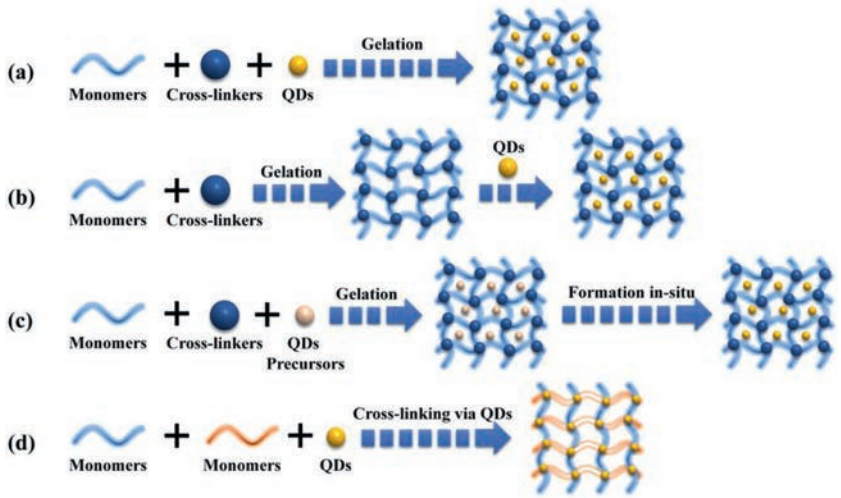

Fig. 2. Four main approaches employed to acquire QDs-hydrogel composites: (a) Hydrogel gelation in a QDs solution; (b) Physically embedding prepared QDs into hydrogels after gelation; (c) Forming QDs *in situ* within the preformed gel; (d) Cross-linking *via* QDs to form hydrogels.

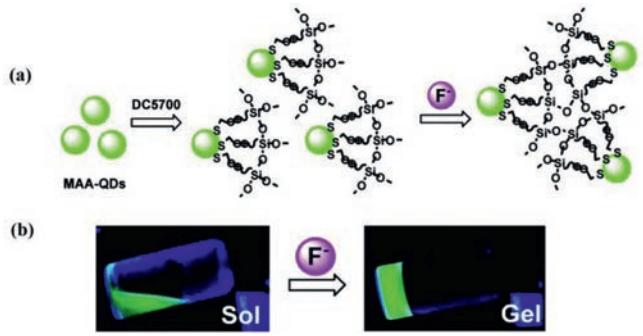

Fig. 3. (a) Schematic diagram of gelation with the introduction of fluoride into the DC5700-QDs System; (b) Sol-gel phase transition of DC5700-QDs solutions with fluoride sodium (λ_{ex} = 365 nm). Copied with permission [45]. Copyright 2018, American Chemical Society.

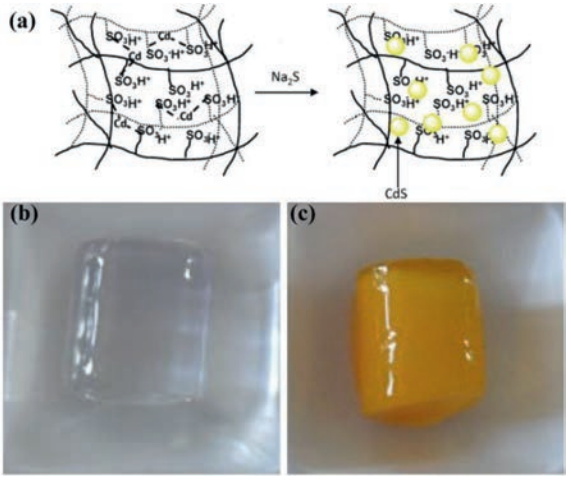

Fig. 5. (a) A schematic diagram of the *in-situ* formation of CdS QDs in a p(AMPS) hydrogel; (b) Photo of bare p(AMPS); (c) Photo of p(AMPS)-CdS QDs. Reproduced with permission [49]. Copyright 2011, Elsevier. B.V.

poly(2-acrylamido-2-methyl-1-propansulfonic acid) [p(AMPS)] hydrogels tended to absorb the Cd^{2+} from aqueous environments through electrostatic interactions. When the p(AMPS) hydrogels were transferred into the Na_2S solution, the outer periphery turned from transparent to light yellow color, indicating the successful preparation of CdS QDs *in situ* (Fig. 5). Similarly, Yang *et al.* [50] reported an irradiation induced reduction and polymerization-crosslinking method to prepare CdS QDs-hydrogel composites. The *in-situ* growth of CdS QDs were realized through the coordination forces with amino groups, and thus improving the stability and durability of CdS QDs in the composite. The CdS QDs were well-dispersed in the hydrogel with a size distribution between 4.1 nm

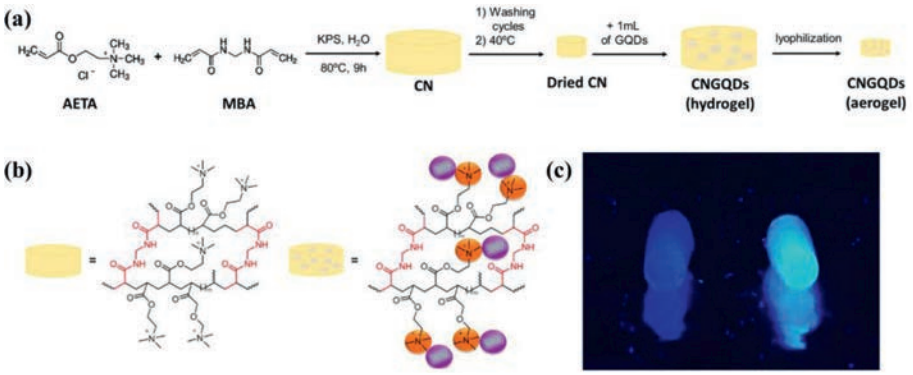

Fig. 4. (a) Preparation process of GQDs-hydrogel (CNGQDs); (b) Chemical structure of the chemically cross-linked hydrogel (CN) and CNGQDs; (c) Photo of CN (left) and CNGQDs (right) (λ_{ex} = 365 nm). Reproduced with permission [47]. Copyright 2018, American Chemical Society.

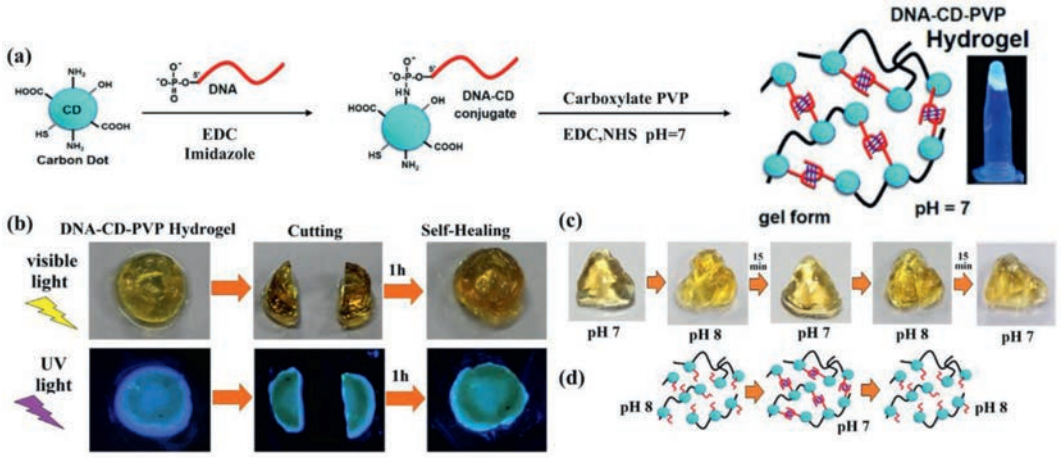

Fig. 6. (a) A pictorial representation for the synthesis of DNA-CD-PVP hydrogels from CDs, DNA, carboxylate PVP; (b) Images presenting the self-healing process; (c) Images presenting the shape memory; (d) A pictorial diagram for the retention of shape of the hydrogel at pH 7. Reproduced with permission [51]. Copyright 2019, American Chemical Society.

and 4.9 nm, which were confirmed with the electron microscopy results. In this synthetic process, the stable 3D structure of hydrogels can provide necessary physical and chemical functions for crystal growth of QDs. A certain volume limitation makes it possible to control the *in-situ* growth of QDs in the corresponding hydrogel systems.

2.4. Cross-linking via QDs to form hydrogels

In addition, a special example to develop QDs-hydrogel composites involves the cross-linking groups on the surface of QDs. Nayak *et al.* [51] produced a pH-responsive hybrid hydrogel using carbon dots (CDs) as the common nucleus, with a single-strand DNA and PVP simultaneously conjugated to a single CD (Fig. 6a). The dual conjugation infused the resulting hydrogel with increased mechanical strength and self-healing properties (Fig. 6b). With the pH decreased, the DNA-CD-PVP conjugate transformed from sol state to gel state due to the formation of intermolecular I-motif, and thus realizing the pH responsiveness (Figs. 6c and d). Compared to the traditional hydrogels, the ability to form multiple bonds in the gel networks may be the main advantages of using QDs as crosslinking agents [20]. In this approach, the functional groups on the surface of QDs participate in cross-linking, thus QDs are part of hydrogels and influence the morphology of the hydrogels. Therefore, adjusting the functional groups of the QDs and the ratio of the monomers to QDs is of great significance to adjust the properties of the composites.

3. QDs-hydrogel composites for biomedical application

The combination of QDs and hydrogels endows the composites synergistic, unique and useful properties that are not simultaneously found in the individual components [20]. Owing to the advantages of 3D structure, high water content and biocompatibility, QDs-hydrogel composites can mimic human tissue microenvironment. Also, the adjustability of their physical and chemical properties allows them to show great potential in biomedical applications, which can be specifically divided into bioimaging, biosensing and drug delivery. Different types of QDs-hydrogel composites and their applications are described below.

3.1. Biosensing

Biosensing is an advanced technology in the biomedical field involving kinds of biosensors based on biologically-derived sensitive element. The application of nanotechnology in biosensing has aroused increasing interest due to the advantages of high solubility, low toxicity, and excellent biodegradability. As advanced immobilization materials, QDs-hydrogel composites endow biosensors with the ability to work under extreme circumstances.

3.1.1. Biological stimuli sensing

QDs-hydrogel composites may go through structural or morphological changes when stimulated by external biological stimuli. These responses can be utilized to sense biological stimuli like pH [52,53], temperature [54], pressure [55], *etc.* Ryplida *et al.* [55] demonstrated the use of a hydrogel-based biosensor for monitoring continuous human motion *via* pressure sensing. The hydrogel was synthesized by combining CDs with a polyvinyl alcohol (PVA) and catechol-conjugated chitosan hydrogel matrix. Here, the hydrophobicity of loaded CDs had a great influence on mechanical properties, electronic signal acquisition and ability of shape recovery. External pressure brought about a deformation in the structure of hydrogel, leading to the change in its conductivity way and the output electronic signal (Fig. 7a). After removing the external pressure, the output electronic signal was refreshed, demonstrating the reversibility under external pressure (Fig. 7b). Based on the unique electrical and mechanical properties under pressure stimulation, the prepared hydrogel composite can be applied to study and assess the vibration in the process of speaking and breathing, to achieve the purpose of continuously monitoring human motion as a biosensor (Figs. 7c-e).

3.1.2. Bio-ion sensing

Besides biological stimuli, QDs-hydrogel composites can also be used in ion detection, like heavy metal ions [56] and oxygen radicals [57]. Gogoi *et al.* [56] reported a sensing platform for optical detection of five heavy metal ions based on an agarose hydrogel rooted with CDs, which was prepared *via* the electrostatic interaction between chitosan-based CDs (NH_3^+) and agarose (-OH) (Fig. 8a). When the hydrogel film was immersed in the heavy metal ion solution, the hydrogel film demonstrated a color variation, for instance, Cr^{6+}, Cu^{2+}, Fe^{3+}, Pb^{2+} and Mn^{2+} corresponding to yellow, blue, brown, white and tan brown respectively (Fig. 8c). Meanwhile, the hydrogel film can serve as an effective filter membrane to separate these heavy metal ions. As is shown in the Fig. 8b, CDs showed a good dispersion in agarose hydrogel. The free NH_3^+ group of the CDs went through deprotonation in presence of NaOH, while the deprotonated NH_2 tended to form chelates with

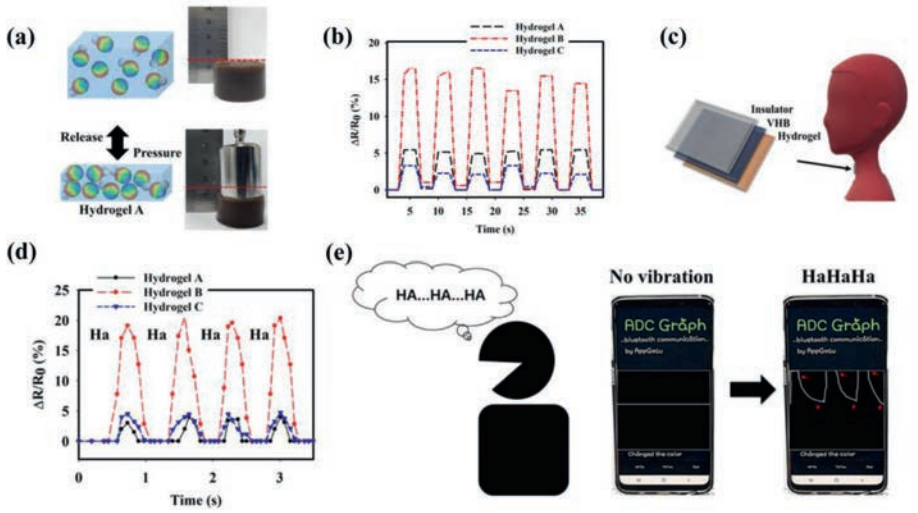

Fig. 7. (a) Pressure-sensing schematic diagrams and photos of prepared hydrogels under a pressing weight of 10 N; (b) Reponses of hydrogel A, B, C in case of repetitive pressure loading/unloading; (c) PVA/C-Chitosan/f-CD hydrogels used for sensing the vocal cord vibration; (d) Resistance response of the prepared PVA/C-Chitosan/f-CD hydrogels when speaking "Ha"; (e) Biosensing process of the speaking of "Ha" using hydrogel B during connection to smartphone. Copied with permission [55]. Copyright 2020, American Chemical Society.

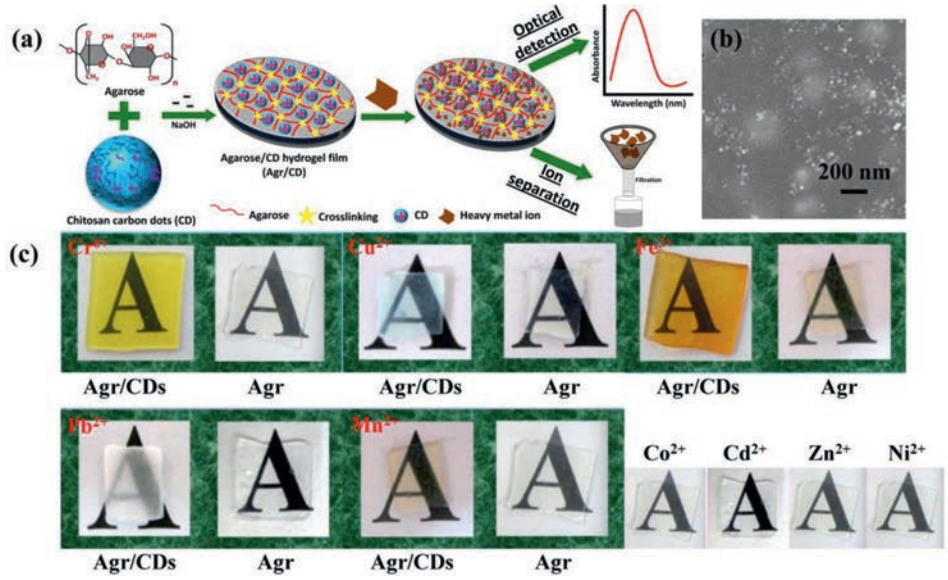

Fig. 8. (a) Schematic presentation upon preparation of agarose/CDs (Agr/CDs) hydrogel film and its application for optical detection and ion separation; (b) SEM image of Agr/CDs; (c) Photos of the color variation of Agr/CDs and Agr when immersed in the heavy metal ion solution (Cr^{6+}, Cu^{2+}, Fe^{3+}, Pb^{2+} and Mn^{2+}). Reproduced with permission [56]. Copyright 2015, American Chemical Society.

heavy metal ions, which displayed the mechanism of sensing and separating the heavy metal ions. As vital trace metal elements, both Cu^{2+} and Fe^{3+} play an important role in biological processes. The detection performance of the mentioned sensing platform underscored the potential for biosensing applications.

3.1.3. Biomolecules sensing

QDs-hydrogel composites can find novel applications in both small and large biological molecules. Target small biological molecules include dopamine [58], glucose [59], progesterone [60], lactate [61] and so forth. Chen *et al.* [60] presented an immobilized QDs-transcription factor-nucleic acid complex to detect progesterone (Fig. 9a). A polyhistidine-tagged transcription factor and a fluorophore-modified cognate DNA were embedded in an optically transparent, soft and flexible hydrogel, which allowed the analyte progesterone to pass freely (Fig. 9b). The device was integrated of biorecognition element(s) and transduction mechanism, suited for real-time monitoring, repeated measurements (Fig. 9c).

Target large biological molecules include RNA [62], DNA [63], enzyme [64,65], *etc.* Mohammadi *et al.* [62] used the Schiff base reaction among the amine in chitosan and aldehyde groups on the CDs surface to form fluorescent hydrogels. The CDs embedded in hydrogel allowed for the selective sensing/identification of microRNA-21, which can be sensed by photoluminescence intensity. In presence of microRNA-21, the interaction of the fluorophore with microRNA-21 led to the radiationless deactivation to ground of the fluorophore. This shift was the outcome of the surface quenching states of CDs. The extent of fluorescence quenching confirmed the microRNA-21 recognition and quantification of its concentration. When different concentrations of microRNA-21 were added to the hydrogel, the PL intensity decreased linearly with the logarithm of microRNA-21 concentration within a certain

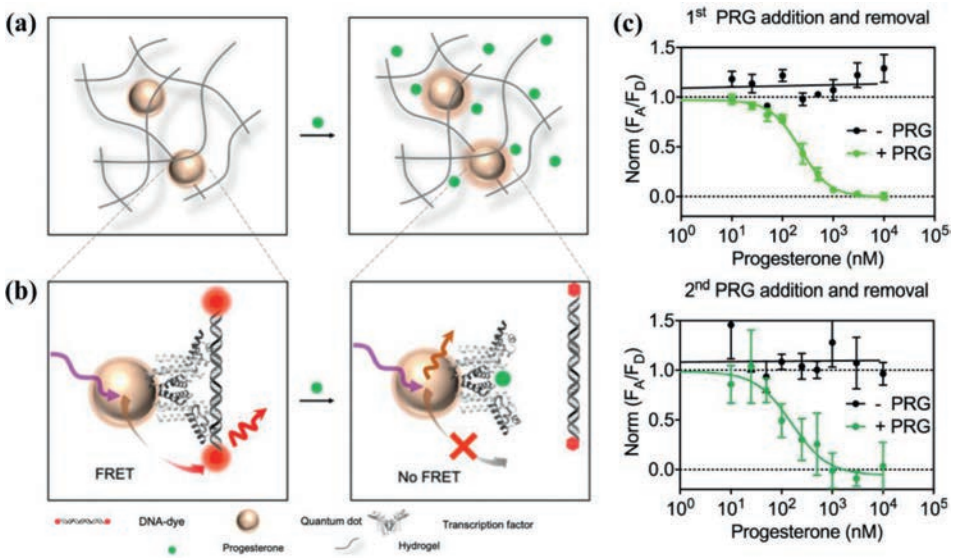

Fig. 9. (a) Pictorial representation upon the diffusion of progesterone in QDs-hydrogel composites; (b) The transcription factors-DNA binding mechanism used in progesterone sensing; (c) Sensing response during the first and second cycle of the exposure and removal of progesterone (Green: exposure, Black: removal). Copied with permission [60]. Copyright 2020, American Chemical Society.

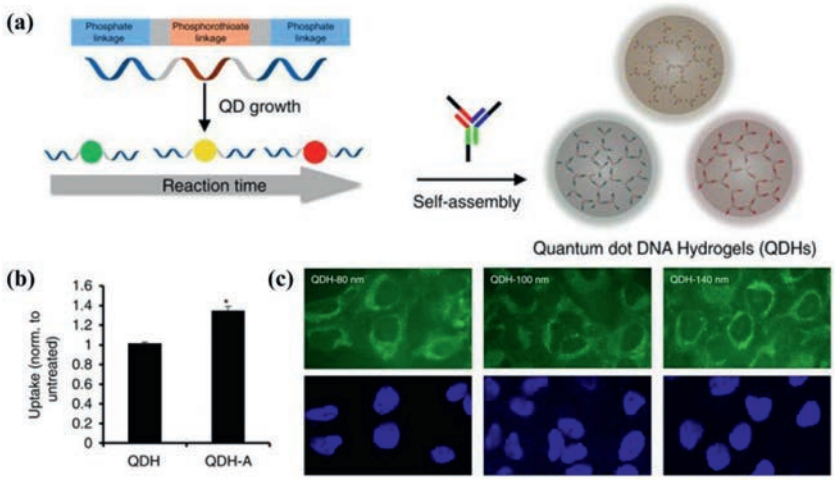

Fig. 10. (a) Schematic representations of preparation process of the self-assembled QDs DNA hydrogels (QDHs); (b) Confocal microscopy images of Hela cells incubated with 80 nm, 100 nm, and 140 nm QDH (green), nuclei (blue); (c) Uptake of QDH and QDH-aptamer *via* flow cytometry. Copied with permission [37]. Copyright 2017, The Author(s).

range. The authors have thus exploited the ability of the hydrogels to respond to microRNA-21 through fluorescence quenching.

3.2. Bioimaging

Bioimaging is a process of visualizing and analyzing the biological process *in vivo* qualitatively and quantitatively. It can also be combined with other biological tools to achieve rapid visualization based on molecules for further applications in cancer diagnosis and therapy [66]. Thanks to the excellent biocompatibility, optical stability and low toxicity, QDs-hydrogel composites attract increasing research interest as bioimaging probes [67-70].

As it was demonstrated by several studies, the fluorescent properties of QDs-hydrogel composites can be the most commonly used ones in bioimaging. Zhang with his group [37] has done excellent work on the development and design of CdTe QDs DNA hydrogels for bioimaging. The DNA hydrogel network was prepared entirely through self-assembly, leveraging the DNA complementarity (Fig. 10a). The size of QDs hydrogels can be tuned to be tailored for specific applications. In addition, they introduced multifunctionality of cell-specific targeting through the DNA-guided interactions, functionalizing QDs hydrogels with aptamers to target specific cell types (Fig. 10b). The QDs DNA hydrogels have shown immense potential in multiplexed imaging studies and rationally-designed synergistic biomedical functionality (Fig. 10c). However, cadmium-free QDs like CDs are relatively lower-cytotoxicity than cadmium-containing ones. Wang *et al.* [71] took CDs as fluorescent indicator to prepare QDs-hydrogel composites. The direct embedding of CDs avoided chemically bonding, allowing low photobleaching and good biocompatibility. The embedded CDs in hydrogels diffused outside in case of hydrogel degradation, which can be utilized to describe the degradation process in real time and noninvasively by fluorescence-related tracking and monitoring. This fluorescence-related visual bioimaging methodology provided convenience for the rational design of biodegradable injectable hydrogels.

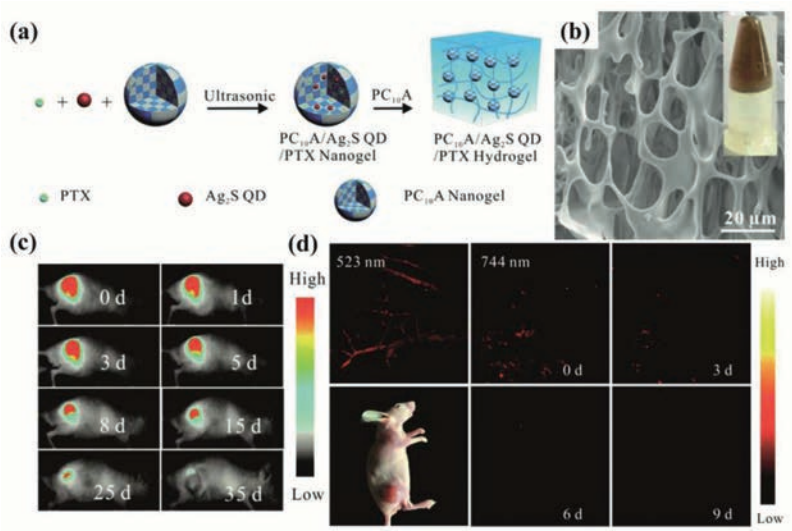

Fig. 11. (a) Pictorial illustration of the fabrication of the $PC_{10}A/Ag_2S$ QDs/PTX hydrogels; (b) SEM image and photo (inset) of the $PC_{10}A/Ag_2S$ QDs/PTX hydrogels; (c) Fluorescence imaging of mice that injected with 100 μL of the $PC_{10}A/Ag_2S$ QDs/PTX hydrogel; (d) PA imaging of the tumor site that injected with 100 uL of the $PC_{10}A/Ag_2S$ QDs/PTX hydrogel (λ_{ex}= 744 and 523 nm). Copied with permission [73]. Copyright 2019, Royal Society of Chemistry.

Besides fluorescent properties, other properties can be also used to rationally design multifunctional hydrogel probes, like magnetic and photothermal properties. Shen *et al.* [72] prepared the chitosan-based luminescent/magnetic nanomaterials by direct gelation of chitosan, with CdTe QDs and superparamagnetic iron oxide embedded inside. By changing temperature, pH and reaction time, the vibrating modes and the feeding ratios of chitosan/QDs/magnetic nanoparticles, the morphologies and properties can be significantly tailored. Capable of being successfully transported into cells by endocytosis, the hybrid nanogels can serve as a multifunctional luminescent/magnetic probe for bioimaging. Jin *et al.* [73] designed and synthesized a novel type of injectable hydrogel based on genetically engineered polypeptide which could serve as a photothermal therapy agent. Both hydrophobic Ag_2S QDs and paclitaxel (PTX) were encapsulated in hydrogels to prepare multifunctional $PC_{10}A/Ag_2S$ QDs/PTX hydrogels of good biocompatibility (Figs. 11a and b). The slow degradation of $PC_{10}A$ hydrogels enabled the continuous release of paclitaxel. The NIR emission and high photothermal effect of Ag_2S QDs provided the hydrogels with powerful photothermal therapeutic capacities for tumor treatment, which were proved *in vitro* and *in vivo*. The merging of fluorescent and photoacoustic imaging can make up for the deficiency of individual imaging, possessing microscopic spatial resolution and macroscopic ultrasensitivity (Figs. 11c and d).

3.3. Drug delivery

Drug delivery is another vital application in the biomedicine field. As an emerging drug carrier, hydrogels have been widely applied in the drug delivery area. Compared to nanoparticle carriers, hydrogels have advantages in their less severe side effects, good biocompatibility and biodegradability. Hydrogels can respond to some stimuli (pH, temperature or else) and achieve the controllable release of drugs, while the addition of QDs helps track the hydrogel dissolution and drug loading in hydrogel [74-76].

Singh *et al.* [77] utilized the low extracellular pH in the tumor microenvironment to develop a DNA-CDs hybrid hydrogel. CDs and chemotherapeutic drug Doxorubicin (DOX) were encapsulated in the hydrogels, which acted as a container for sustained release for the drug (Fig. 12a). In addition to acting as a cross-linker for network formation, CDs also helped encapsulate drugs with DNA through electrostatic action. When the pH of the solution altered from alkaline to acidic, the DNA-CDs hybrid hydrogel underwent a sol-gel transition (Fig. 12b). The presence of CDs made it possible to track the hydrogel dissolution and drug loading (Fig. 12c). When cell viability tests were carried out in Hela cells, the hybrid hydrogels could effectively kill Hela cells in presence of the Dox-loaded hydrogels due to the damaging effect of acidic pH on hydrogels (Fig. 12d).

Yang *et al.* [32] developed a new type of multifunctional QDs-polypeptide hybrid hydrogel through the self-assembly between artificial polypeptides and CdSe-ZnS core-shell QDs. There was a tunable sandwich-like structure on the surface of QDs consisting of two hydrophobic layers and one hydrophilic layer between them, which endowed the hybrid hydrogels with the ability to load hydrophobic and hydrophilic drugs simultaneously. Coiled-coil polypeptides probably demonstrate conformational transitions in response to pH, temperature, ionic strength or solvents. Thus, the drug release process of the drug-loaded QDs-polypeptide nanogels *in vitro* varied significantly with temperature, pH and competitors. The arginine-glycine-aspartic acid motif embedded in the hydrogels realized the selective combination with integrin $\alpha_v\beta_3$ and also the targeting ability. The combination of these functions made the QDs-polypeptide hybrid hydrogel a potentially viable tool for cancer diagnosis, imaging and therapy.

Apart from responding to physiological stimuli, hydrogels were expected to work toward providing a therapeutic effect. Recently, Xiang *et al.* [78] pioneered CDs/ZnO decorated folic acid-conjugated polydopamine hydrogel through the rapid assembly of dopamine and folic acid cross-linked by transition metal ions. In presence of Zn^{2+} and polydopamine, the prepared hybrid hydrogel can be applied in anti-bacterial infection. The carboxyl groups in the FA molecule and catechol in polydopamine tended to chelate Zn^{2+} to form metal-ligand coordination, which enabled the injectable hydrogel to match with the shape of the wound. The polydopamine coated inside was capable of generating reactive oxygen species and heating under illumination, endowing the hybrid hydrogels with an excellent antibacterial capability. A preliminary *in vitro* antibacterial test indicated that the injectable hydrogel could continuously release Zn^{2+}, bringing about a sustained antimicrobial effect and promoted fibroblast growth. Thus, the prepared hydrogel showed potential for the reconstruction of bacteria-infected tissues.

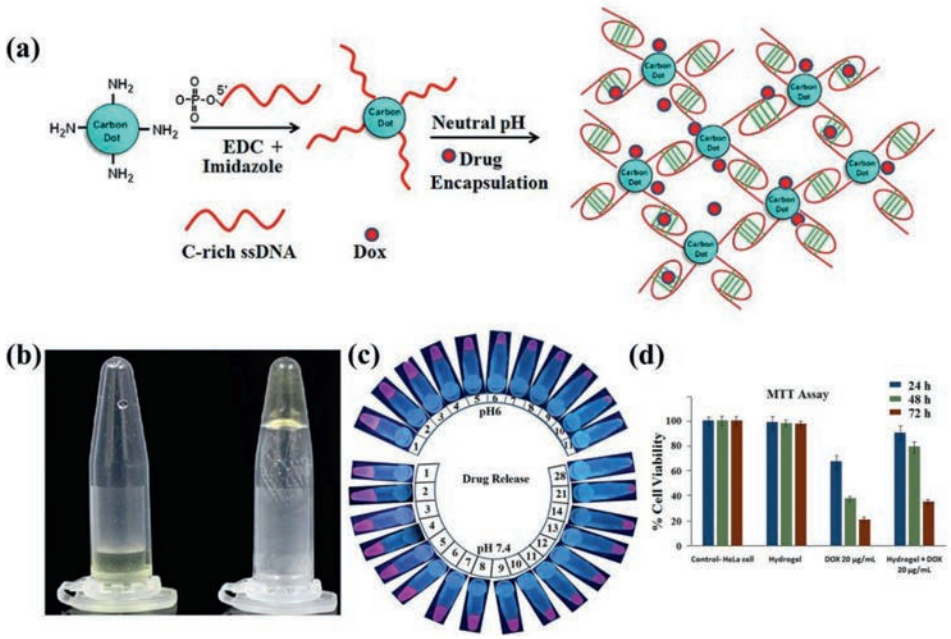

Fig. 12. (a) Schematic illustrations for the fabrication of the DOX-encapsulated DNA-CDs hybrid hydrogels; (b) Photos of the sol-gel transition of DNA-CDs in white light; (c) Photos of the drug release of DNA-CDs hybrid hydrogels in PBS buffer at pH 7.4 and 6 with time; (d) Cell viability of HeLa cells treated with DNA-CDs hydrogel, free Dox and Dox encapsulated DNA-CDs hydrogel. Copied with permission [77]. Copyright 2016, Elsevier Ltd.

4. Conclusion and outlook

In this review, we have summarized synthesis methods of QDs-hydrogel composites into four categories and also given an overview of their applications in the biomedical fields such as bioimaging, biosensing and drug delivery. QDs-hydrogel composites have appealed to researchers from different fields due to their unique properties, which can undoubtedly be promising candidates in biomedical fields. However, there are still some challenges in their preparation and application as follows despite the advanced properties of QDs-hydrogel composites.

Firstly, the properties of QDs-hydrogel composites cannot be precisely designed. Although the formation of hydrogels has been carefully designed, QDs tend to aggregate in the hydrogel framework, leading to fluorescence quenching. Therefore, the photoluminescence quantum yield of the QDs is usually higher than the upper bound of the QDs-hydrogel composites [79], and the emission wavelength also alters, which influences the optical properties of the composites. QDs are often applied to enhance the mechanical and solubility properties, while few studies have focused on the modulation and improvement of the properties of QDs by utilizing the hydrogel matrix. For example, the *in-situ* growth of QDs can be restricted by the pore size of hydrogels to obtain QDs with uniform size, or the functional groups on the surface of QDs can be modified by hydrogels. Computer simulation has been employed in several literatures to investigate the combining mechanism and the properties of composites [80-84]. Thus, optimizing the design of QDs-hydrogel composites with the aid of computer simulation is of great significance.

As biomedical applications are usually *in vivo*, the biocompatibility of QDs-hydrogel composites should be of great importance [85]. Multiple toxicity tests are required to ensure the reliability of the composites, prolonging the time from laboratory research to clinical applications, so the composites are required to produce few harmful wastes or the produced wastes can be discharged efficiently, and rapid toxicity screening are needed to shorten the process to clinical applications. Also, hydrogels tend to lack stability and durability *in vivo*, which will limit their repeatability and recyclability. Therefore, the ideal hydrogel framework should possess excellent mechanical stability and low biotoxicity. Furthermore, the hydrogels applied in bioimaging and biosensing should have strong interaction with the embedded QDs, thus QDs can still be maintained in the hydrogel framework despite the changes of the biological environment.

Most of the applications of QDs-hydrogel composites focus on their fluorescent properties, while less applications utilizing other properties (magnetic, photothermal, *etc.*), let alone bimodal applications. However, the scattering and absorption of light by biological molecules may be another most important challenge in fluorescence imaging. Due to deeper light penetration to biological systems, near-infrared light can be a viable alternative for bioimaging [86-88]. Utilizing magnetic or photothermal properties simultaneously is also effective [89-91]. Hence, the design of near-infrared-emissive or bimodal QDs-hydrogel composites will greatly broaden their biomedical applications.

Declaration of competing interest

The authors declare that they have no known competing financial interests or personal relationships that could have appeared to influence the work reported in this paper.

Acknowledgments

This work was supported by the National Natural Science Foundation of China (NSFC, Nos. 62074044, 61904036 and 61675049), Zhongshan-Fudan Joint Innovation Center and Jihua Laboratory Projects of Guangdong Province (No. X190111UZ190).

References

[1] K.H. Bae, M. Kurisawa, Biomater. Sci. 4 (2016) 1184–1192.
[2] N. Mehwish, X. Dou, Y. Zhao, C. Feng, Mater. Horiz. 6 (2019) 14–44.
[3] Y.Q. Li, D.J. Young, X.J. Loh, Mater. Chem. Front. 3 (2019) 1489–1502.
[4] A. Jayakumar, V.K. Jose, J.M. Lee, Small Methods 4 (2020) 1900735.
[5] H. Dai, Y. Chen, W. Dai, et al., Adv. Mater. 33 (2021) 2101239.
[6] M. Hasanzadeh, N. Shadjou, M. de la Guardia, TrAC Trends Anal. Chem. 102 (2018) 210–224.

[7] M. Chan, A. Almutairi, Mater. Horiz. 3 (2016) 21–40.
[8] L. Yu, J.D. Ding, Chem. Soc. Rev. 37 (2008) 1473–1481.
[9] J. Shi, Z. Shi, Y. Dong, F. Wu, D. Liu, ACS Appl. Bio Mater. 3 (2020) 2827–2837.
[10] S. Park, K.M. Park, Polymers 8 (2016) 8010023.
[11] O. Wichterle, D. Lim, Nature 185 (1960) 117–118.
[12] H. Dai, Y. Chen, W. Dai, et al., Adv. Mater. Technol. 6 (2021) 2000848.
[13] D. Gan, T. Xu, W. Xing, et al., Adv. Funct. Mater. 29 (2019) 1805964.
[14] L. Han, X. Lu, K. Liu, et al., ACS Nano 11 (2017) 2561–2574.
[15] C. Ma, W. Lu, X. Yang, et al., Adv. Funct. Mater. 28 (2018) 1704568.
[16] C. Li, S. Zheng, C. Du, et al., ACS Appl. Polym. Mater. 2 (2020) 1043–1052.
[17] T.H. Kim, J. Seo, S.J. Lee, et al., Chem. Mater. 19 (2007) 5815–5817.
[18] H. Cai, P. Yao, Nanoscale 5 (2013) 2892–2900.
[19] P. Thoniyot, M.J. Tan, A.A. Karim, D.J. Young, X.J. Loh, Adv. Sci. 2 (2015) 1400010.
[20] K. Lei, Q. Ma, L. Yu, J. Ding, J. Mater. Chem. B 4 (2016) 7793–7812.
[21] B. Sui, Y. Li, B. Yang, Chin. Chem. Lett. 31 (2020) 1443–1447.
[22] J. Bai, J. Chu, X. Yin, et al., Chem. Eng. J. 391 (2020) 123553.
[23] A.J. Sutherland, Curr. Opin. Solid ST. M. 6 (2002) 365–370.
[24] K. Kalyanasundaram, E. Borgarello, D. Duonghong, M. Gratzel, Angew. Chem. Int. Ed. 20 (1981) 987–988.
[25] Z. Hu, H. Dai, X. Wei, et al., RSC Adv. 10 (2020) 17266–17269.
[26] W. Zhang, X. Zhou, X. Zhong, Inorg. Chem. 51 (2012) 3579–3587.
[27] R. Zeng, R. Shen, Y. Zhao, et al., Nanotechnology 25 (2014) 135602.
[28] J. Wei, Z. Hu, W. Zhou, et al., J. Colloid Interface Sci. 602 (2021) 307–315.
[29] B. Wang, J. Li, Z. Tang, B. Yang, S. Lu, Sci. Bull. 64 (2019) 1285–1292.
[30] S. Lu, L. Sui, J. Liu, et al., Adv. Mater. 29 (2017) 1603443.
[31] W. Li, Y. Liu, B. Wang, et al., Chin. Chem. Lett. 30 (2019) 2323–2327.
[32] J. Yang, M. Yao, L. Wen, et al., Nanoscale 6 (2014) 11282–11292.
[33] J. Zhang, J. Jin, J. Wan, et al., Chem. Eng. J. 408 (2021) 127351.
[34] A. Nair, J. Shen, P. Thevenot, et al., Nanotechnology 19 (2008) 485102.
[35] L. Zhou, F. Zhang, Mater. Sci. Eng. C 31 (2011) 1429–1435.
[36] J. Yuan, D. Wen, N. Gaponik, A. Eychmuller, Angew. Chem. Int. Ed. 52 (2013) 976–979.
[37] L. Zhang, S.R. Jean, S. Ahmed, et al., Nat. Commun. 8 (2017) 381.
[38] C. Lee, B. Pant, B.S. Kim, et al., Mater. Lett. 207 (2017) 57–61.
[39] L. Ai, Y. Yang, B. Wang, et al., Sci. Bull. 66 (2021) 839–856.
[40] K. Deligkaris, T.S. Tadele, W. Olthuis, A. van den Berg, Sens. Actuators B: Chem. 147 (2010) 765–774.
[41] C. Liu, F. Li, J. Yang, F. Tian, J. Sun, J. Control. Release 213 (2015) E16–E17.
[42] B.W. Garner, T. Cai, Z.B. Hu, A. Neogi, Opt. Express 16 (2008) 19410–19418.
[43] M. Hu, X.Y. Gu, Y. Hu, Y.H. Deng, C.Y. Wang, Macromol. Mater. Eng. 301 (2016) 1352–1362.
[44] S.A. Park, E. Jang, W.G. Koh, B. Kim, Talanta 84 (2011) 1000–1003.
[45] J. Zhou, H. Li, ACS Appl. Mater. Interfaces 4 (2012) 721–724.
[46] J.H. Holtz, S.A. Asher, Nature 389 (1997) 829–832.
[47] A. Martin-Pacheco, A.E. Del Rio Castillo, C. Martin, et al., ACS Appl. Mater. Interfaces 10 (2018) 18192–18201.
[48] J. Yang, S. Zhao, R. Jin, et al., Macromol. Mater. Eng. 304 (2019) 1800658.
[49] N. Sahiner, K. Sel, K. Meral, et al., Colloids Surf. A 389 (2011) 6–11.
[50] T. Yang, Q. Li, W. Wen, et al., Radiat. Phys. Chem. 145 (2018) 130–134.
[51] S. Nayak, S.R. Prasad, D. Mandal, P. Das, ACS Appl. Bio Mater. 3 (2020) 7865–7875.
[52] W. Wu, J. Shen, P. Banerjee, S. Zhou, Biomaterials 31 (2010) 8371–8381.
[53] W. Wu, M. Aiello, T. Zhou, A. Berliner, P. Banerjee, S. Zhou, Biomaterials 31 (2010) 3023–3031.
[54] J.H. Yoo, S.W. Lee, J. Nanosci. Nanotechnol. 14 (2014) 7648–7653.
[55] B. Ryplida, I. In, S.Y. Park, ACS Appl. Mater. Interfaces 12 (2020) 51766–51775.
[56] N. Gogoi, M. Barooah, G. Majumdar, D. Chowdhury, ACS Appl. Mater. Interfaces 7 (2015) 3058–3067.
[57] S. Bhattacharya, R. Sarkar, S. Nandi, A. Porgador, R. Jelinek, Anal. Chem. 89 (2017) 830–836.
[58] P.K. Pandey, K.Rawat Preeti, T. Prasad, H.B. Bohidar, J. Mater Chem. B 8 (2020) 1277–1289.
[59] H.I. Park, S.Y. Park, ACS Appl. Mater. Interfaces 10 (2018) 30172–30179.
[60] M. Chen, C. Grazon, P. Sensharma, et al., ACS Appl. Mater. Interfaces 12 (2020) 43513–43521.
[61] X. Zhang, S. Ding, S. Cao, A. Zhu, G. Shi, Biosens. Bioelectron. 80 (2016) 315–322.
[62] S. Mohammadi, S. Mohammadi, A. Salimi, Talanta 224 (2021) 121895.
[63] Y. Zhao, X. Zhao, B. Tang, et al., Adv. Funct. Mater. 20 (2010) 976–982.
[64] C. Ruiz-Palomero, S. Benitez-Martinez, M.L. Soriano, M. Valcarcel, Anal. Chim. Acta 974 (2017) 93–99.
[65] J.H. Kim, S.Y. Lim, D.H. Nam, et al., Biosens. Bioelectron. 26 (2011) 1860–1865.
[66] R. Abbel, R. van der Weegen, W. Pisula, et al., Chem. Eur. J. 15 (2009) 9737–9746.
[67] Y. Wang, Y. Xue, J. Wang, et al., J. Polym. Res. 26 (2019) 248.
[68] N.S. Rejinold, K.P. Chennazhi, H. Tamura, S.V. Nair, J. Rangasamy, ACS Appl. Mater. Interfaces. 3 (2011) 3654–3665.
[69] D. Zhao, W. Ma, R. Wang, et al., Polymers 11 (2019) 1171.
[70] Y. Liu, J. Yang, P. Zhang, C. Liu, W. Wang, W. Liu, J. Mater. Chem. 22 (2012) 512–519.
[71] L. Wang, B. Li, F. Xu, et al., Biomaterials 145 (2017) 192–206.
[72] J. Shen, L. Xu, Y. Lu, et al., Int. J. Pharm. 427 (2012) 400–409.
[73] R. Jin, X. Yang, D. Zhao, et al., Nanoscale 11 (2019) 16080–16091.
[74] H. Lu, L. Lv, J. Ma, et al., J. Mech. Behav. Biomed. Mater. 88 (2018) 261–269.
[75] N. Sarkar, G. Sahoo, R. Das, G. Prusty, S.K. Swain, Eur. J. Pharm. Sci. 109 (2017) 359–371.
[76] S. Javanbakht, H. Namazi, Mater. Sci. Eng. C 87 (2018) 50–59.
[77] S. Singh, A. Mishra, R. Kumari, et al., Carbon 114 (2017) 169–176.
[78] Y. Xiang, C. Mao, X. Liu, et al., Small 15 (2019) 1900322.
[79] A.P. Alivisatos, Science 271 (1996) 933–937.
[80] Y. Zhao, R. Yang, W. Wan, et al., Chem. Eng. J. 389 (2020) 124453.
[81] X. Wang, X. Li, N. Chen, et al., NPJ Comput. Mater. 31 (2020) 6.
[82] F. Mekki-Berrada, Z. Ren, T. Huang, et al., NPJ Comput. Mater. 7 (2021) 55.
[83] N. Marzari, A. Ferretti, C. Wolverton, Nat. Mater. 20 (2021) 736–749.
[84] S.G. Louie, Y.H. Chan, F.H. da Jornada, Z. Li, D. Qiu, Nat. Mater. 20 (2021) 728–735.
[85] C.E. Bradburne, J.B. Delehanty, K.B. Gemmill, et al., Bioconjugate Chem. 24 (2013) 1570–1583.
[86] M.T. Hasan, B.H. Lee, C.W. Lin, et al., 2D Mater. 8 (2021) 035013.
[87] M.A. Krishnan, K. Yadav, P. Roach, V. Chelvam, Biomater. Sci. 9 (2021) 2295–2312.
[88] X. Dong, H. Zhao, Y. Mi, et al., Chin. Chem. Lett. 31 (2020) 1616–1619.
[89] D. Zhao, J. Yang, R. Xia, et al., Chem. Commun. 54 (2018) 527–530.
[90] J. Zhang, C. Hu, B. Zhang, Nanomedicine 12 (2016) 505 505.
[91] Y. Yang, L. Lin, L. Jing, X. Yue, Z. Dai, ACS Appl. Mater. Interfaces 9 (2017) 23450–23457.